


RESEARCH REPORT

WILEY

A novel de novo variant in *POLR3B* gene associated with a primary axonal involvement of the largest nerve fibers

Alessandro Geroldi¹  | Stefano Tozza²  | Chiara Fiorillo^{1,3} | Maria Nolano² | Paola Fossa⁴ | Floriana Vitale² | Regi Domi⁴ | Andrea Gaudio⁵ | Alessia Mammi¹ | Serena Patrone¹ | Andrea La Barbera⁵ | Paola Origone^{1,5} | Clarissa Ponti^{1,5} | Francesca Sanguineri^{1,5} | Federico Zara^{1,6} | Matteo Cataldi^{1,3} | Vincenzo Salpietro^{1,6} | Consuelo Barbara Venturi⁷ | Sara Massucco^{1,8} | Angelo Schenone^{1,8} | Fiore Manganelli² | Paola Mandich^{1,5} | Emilia Bellone^{1,5} | Fabio Gotta⁵

¹Department of Neurosciences, Rehabilitation, Ophthalmology, Genetic and Maternal and Infantile Sciences, University of Genoa, Genoa, Italy

²Department of Neuroscience, Reproductive and Odontostomatological Sciences, University of Naples Federico II, Naples, Italy

³Child Neuropsychiatric Unit, IRCCS Institute G. Gaslini, Genoa, Italy

⁴Department of Pharmacy, University of Genoa, Genoa, Italy

⁵OU Medical Genetics, IRCCS Ospedale Policlinico San Martino, Genoa, Italy

⁶Medical Genetic Unit, IRCCS Institute G. Gaslini, Genoa, Italy

⁷OU Pathological Anatomy, IRCCS Ospedale Policlinico San Martino, Genoa, Italy

⁸OU Neurology Clinic, IRCCS Ospedale Policlinico San Martino, Genoa, Italy

Correspondence

Emilia Bellone, Department of Neuroscience, Rehabilitation, Ophthalmology, Genetics and Maternal and Child Health, Section of Medical Genetics, University of Genoa, 16132 Genoa, Italy.

Email: ebellone@unige.it

Present address

Vincenzo Salpietro, Department of Biotechnological and Applied Clinical Science, University of L'Aquila, L'Aquila, Italy.

Abstract

Background and Aims: *POLR3B* gene encodes a subunit of RNA polymerase III (Pol III). Biallelic mutations in *POLR3B* are associated with leukodystrophies, but recently de novo heterozygous mutations have been described in early onset peripheral demyelinating neuropathies with or without central involvement. Here, we report the first Italian case carrying a de novo variant in *POLR3B* with a pure neuropathy phenotype and primary axonal involvement of the largest nerve fibers.

Methods: Nerve conduction studies, sympathetic skin response, dynamic sweat test, tactile and thermal quantitative sensory testing and brain magnetic resonance imaging were performed according to standard procedures. Histopathological examination was performed on skin and sural nerve biopsies. Molecular analysis of the proband and his relatives was performed with Next Generation Sequencing. The impact of the identified variant on the overall protein structure was evaluated through rotamers method.

Results: Since his early adolescence, the patient presented with signs of polyneuropathy with severe distal weakness, atrophy, and reduced sensation. Neurophysiological studies showed a sensory-motor axonal polyneuropathy, with confirmed small fiber involvement. In addition, skin biopsy and sural nerve biopsy showed predominant large fibers involvement. A trio's whole exome sequencing revealed a novel de novo variant p.(Arg1046Cys) in *POLR3B*, which was classified as Probably Pathogenic. Molecular modeling data confirmed a deleterious effect of the variant on protein structure.

Interpretation: Neurophysiological and morphological findings suggest a primary axonal involvement of the largest nerve fibers in *POLR3B*-related neuropathies. A partial loss of function mechanism is proposed for both neuropathy and leukodystrophy phenotypes.

This is an open access article under the terms of the [Creative Commons Attribution-NonCommercial-NoDerivs](https://creativecommons.org/licenses/by-nc-nd/4.0/) License, which permits use and distribution in any medium, provided the original work is properly cited, the use is non-commercial and no modifications or adaptations are made.

© 2023 The Authors. *Journal of the Peripheral Nervous System* published by Wiley Periodicals LLC on behalf of Peripheral Nerve Society.

KEYWORDS

CMT, exome sequencing, large fibers, peripheral neuropathies, POLR3B

1 | INTRODUCTION

Charcot-Marie-Tooth disease (CMT) is a clinically and genetically heterogeneous group of polyneuropathies representing the most common type of inherited peripheral neuropathy.¹

Classically, CMTs are classified into three subgroups based on their neurophysiological features: a demyelinating form (median motor nerve conduction velocity [MNCV] < 38 m/s) and the axonal form (median MNCV > 38 m/s). A third group, referred to as intermediate, has a median MNCV closer to 25–45 m/s.² Additional subtypes are then derived from the neurophysiological classification based on the mode of inheritance and identified molecular defect (<https://neuromuscular.wustl.edu/>).

The *Polymerase III, RNA, subunit B (POLR3B)* gene encodes the second-largest subunit of RNA polymerase III (Pol III), a 17-subunit protein complex involved in the transcription of small non-coding RNAs (such as tRNA, 5S RNA, 7SK RNA, and U6RNA).³

Mutations in Pol III subunits have been associated with a wide spectrum of disorders⁴; in particular, bi-allelic mutations in *POLR3B* are associated with leukodystrophies⁵ and de novo heterozygous mutations have recently been described in peripheral demyelinating neuropathies, classified as CMT1I (CMT demyelinating, autosomal dominant, type I). These patients present with an early onset of peripheral neuropathy, with several additional features, including cerebellar or white matter pathology.^{6–8}

Until today, only eight heterozygous mutations in *POLR3B* have been described in nine unrelated individuals, all of de novo origin.

Here, we report the first Italian case carrying a de novo heterozygous mutation in the *POLR3B* gene (c.3136C>T p.Arg1046Cys) with a pure neuropathy phenotype associated with a primary axonal involvement of the largest nerve fibers.

2 | MATERIALS AND METHODS

2.1 | Clinical evaluation

The patient was evaluated at third-level hospitals (IRCCS Institute “G. Gaslini”, Genoa; University of Naples “Federico II”, Naples) by clinical neurologists, who are experts in hereditary peripheral neuropathies.

Nerve conduction studies were performed according to standard procedures.² To evaluate small fiber functions, sudomotor function was assessed by sympathetic skin response (SSR) and Dynamic Sweat Test (DST),⁹ tactile and thermal (cold and warm) quantitative sensory testing (QST)¹⁰ were performed to estimate large (A β) and small (A δ and C) nerve fibers function, respectively. Cardiovascular (CV) reflexes were assessed according to standard guidelines.¹¹

A brain magnetic resonance imaging (MRI) was performed to evaluate central nervous system involvement. The patient also underwent skin and sural nerve biopsies for histopathological examination.

2.2 | Skin biopsy

Skin biopsies were obtained from the leg, thigh, and fingertip of the V digit using a 3 mm punch. Skin samples were fixed in Zamboni solution and transferred to cryoprotectant solution after 1 h. Free-floating 50 μ m-thick sections were processed for indirect immunofluorescence using a panel of primary antibodies against the following antigens: protein gene product 9.5 (PGP; for neurons), myelin basic protein (MBP; for myelin), vasoactive-intestinal-peptide (for cholinergic fibers), and dopamine-beta-hydroxylase (D β H; for noradrenergic fibers); collagen IV (COLIV for vascular bed and basal membranes). Endothelia and epidermis were labeled with *Ulex europaeus* agglutinin 1. Species-specific secondary antibodies coupled with cyanine 2 and cyanine 3 fluorophores were used. Digital images were captured with a non-laser confocal microscope (Apotome; Zeiss).

2.3 | Sural nerve biopsy

Sural nerve biopsy was obtained from the Achilles tendon insertion under sterile conditions. The specimen was divided into two segments, one of which was fixed in paraformaldehyde, embedded in paraffin, and processed for immunohistochemistry. The other one was fixed in 2.5% glutaraldehyde in cacodylate buffer, pH 7.4, for 24 h and embedded in Epon for light and electron microscopy analyses.

The glutaraldehyde-fixed segment was incubated in 4% osmium tetroxide and then embedded in resin (methacrylate) to obtain semi-thin longitudinal and transversal sections (approximately 1–2 μ m thick), which were stained with toluidine blue for morphological assessment.

Transversal and longitudinal sections stained with hematoxylin-eosin and Congo red, were obtained from the paraformaldehyde fixed nerve segment.

2.4 | Genetic analysis

Written informed consent was obtained from all family members following the Regional Ethical Committee and guidelines for genetic testing used in current clinical practice. This consent allows the anonymous use of the data for research and publication.

The genomic DNA of the proband and his parents was extracted from peripheral blood using standard methods. Preliminary, DNA testing for inherited neuropathies was performed by NGS technology

using an Ampliseq custom gene panel (56 CMT-related genes covering 97.5% at 20× minimum) on an Ion Gene Studio S5 System sequencer (ThermoFisher). Bioinformatic analysis was performed using Ion Reporter (ThermoFisher) and ANNOVAR software. Duplication and deletion of the *PMP22* gene were assessed by multiplex ligation-dependent probe amplification (MLPA) analysis according to the manufactured protocol (MRC Holland-P033 probe mix).

Whole exome sequencing (WES) was performed on trios. Libraries were prepared using the Nextera rapid capture exomes kit (Illumina) and sequenced on an Illumina sequencer (paired-ends 2 × 150). The 85% of the exome was covered with at least 20 reads.

Sequenced reads were aligned to the hg38 reference and annotated using Ensembl Variant Effect Predictor-VEP (<https://www.ensembl.org/info/docs/tools/vep/index.html>).

Variants of interest were selected from those reported in the gnomAD with minor allele frequency <0.01 or not reported at all. In silico functional prediction of variants was evaluated by Revel and BaysDel meta-predictor while HSF (Human Splicing Finder) (<https://www.genomnis.com/access-hsf>), Fruit-Fly (https://www.fruitfly.org/seq_tools/splice.html) and SpliceAI (<https://spliceailookup.broadinstitute.org/>) tools were used to predict the impact of the identified variants on splicing.

2.5 | Molecular modeling

The POLR3 PDB structure was downloaded from the Protein Data Bank (www.rcsb.org, pdb code 7AE1¹²), selecting the structure with the best resolution and the highest number of residues (1–1133 aa, 2.80 Å) among the nine deposited structures.

The residue p.Arg1046 was mutated to Cys using Chimera, selecting the most likely conformation for the side chain¹³ of the cysteine residue which was also used to display hydrogen-bonds.

3 | RESULTS

3.1 | Case report

The proband is a 19-year-old male, the first son of healthy and unrelated parents (Figure 3). While motor development was unimpaired,

he began to show neuromuscular symptoms in early adolescence, with difficulty walking, frequent falls and impaired fine motor skills. At 12 years of age, after a period of immobilization for a left medial malleolus fracture, he noticed calf atrophy and weakness. The first nerve conduction study, performed at the age of 12 years showed a severe sensory-motor polyneuropathy interpreted as demyelinating.

At the last neurological examination, at the age of 19, he presented a bilateral stepping gait, impossible on the feet and heels, moderate weakness, atrophy in the intrinsic hand muscles (more pronounced in the thenar muscles), and severe weakness in the distal muscles of the lower limbs. Sensory examination revealed decreased pinprick and light touch sensation up to the wrist and mid-calf and decreased vibratory sensation to the ankle. Deep tendon reflexes were reduced in the upper limbs and absent in the lower limbs. Severe Achilles tendon retraction was present, whereas no *pes cavus* was evident. Brain MRI showed normal findings without white matter abnormalities.

3.2 | Neurophysiological study

A nerve conduction study performed at the age of 19 years showed absent compound muscle action potential (CMAP) and sensory and action potentials (SAP) in the lower limbs and severe reduction of SAP and CMAP with reduced MNCV and sensory nerve conduction velocity in the upper limbs (Table 1). There was not temporal dispersion or conduction block. According to Berciano and colleagues,² the proximal segment (axilla-elbow) of median nerve recording from pronator teres muscle was performed since the median MNCV was in the range of the intermediate CMT (25–45 m/s) and distal CMAP (dCMAP) was <50% of the lower limit normal value. The proximal segment showed normal CMAP amplitude and MNCV (Table 1), suggesting a predominant axonal neuropathy.

The sudomotor function was severely impaired: SSR was absent, and DST showed a severe reduction in sweat production in both upper and lower limbs. QST revealed abnormal tactile, cold detection threshold, warm detection threshold, cold pain and heat pain, with a length-dependent pattern. Finally, CV reflexes were unchanged.

TABLE 1 Nerve conduction study.

| Nerve | DML (ms) | dCMAP (mV) | Duration (ms) ^a | MCV (m/s) | F-Wave (ms) | SAP (μV) | SCV (m/s) |
|------------------------------|------------------|------------------|----------------------------|------------------|---------------|----------------|------------------|
| Median (from ABP) | 6.1 (4.1) | 2.4 (6.2) | 7 (7.8) | 28.2 (51) | Absent | No | No |
| Median (from pronator teres) | 3.1 (3.5) | 14.2 (6.2) | 10.5 | 55.6 (53) | | | |
| Ulnar (from ADM) | 3.3 (3.1) | 3.3 (7.5) | 5.5 (8.5) | 39.7 (52) | Absent | 1.4 (9) | 33.3 (52) |
| Peroneal | NA | NR | NR | NA | | | |
| Peroneus superficialis | - | - | - | - | | NR | NA |

Note: In bold are reported pathologic values; in the bracket were reported normal value.

Abbreviations: ABP, adductor brevis pollicis; ADM, abductor digiti minimi; dCMAP, distal compound muscle action potential (peak-to-peak); DML, distal motor latency; MCV, motor conduction velocity; NA, not applicable; NR, not recordable; SAP, sensory action potential; SCV, sensory conduction velocity.

^aDuration was calculated as the interval between onset of the first negative peak and return to baseline of the last negative peak.

3.3 | Skin biopsy

Cutaneous innervation showed a severe loss of epidermal nerve fiber (ENF) density with a length-dependent pattern (leg: 2.1 ENF/mm [normal value > 10.9 ENF/mm]; thigh: 6 ENF/mm [normal value > 17.1 ENF/mm]; V digit: 2.6 ENF/mm [normal value > 6.6 ENF/mm]) (Figure 1A). MBP/PGP double stained sections showed a complete absence of myelinated fibers in the leg and very rare dermal myelinated fibers in the thigh and fingertip (Figure 1C). Of interest, the few myelinated fibers were thin and with faint myelin (MBP) staining. In addition, no mechanoreceptors (e.g., Meissner corpuscles and Merkel complexes) and intrapapillary myelinated endings were found in the glabrous skin sections (Figure 1C). Finally, the annessial innervation showed a moderate loss of cholinergic fibers around sweat glands and a mild reduction of adrenergic fibers along the pilomotor muscles.

3.4 | Sural nerve biopsy

Examination of the sural nerve biopsy showed a diffuse reduction in the density of large, myelinated fibers. Several small, myelinated fibers sometimes surrounded by thin myelin were observed. The density of small myelinated and unmyelinated fibers was preserved. Fibers undergoing active axonal degeneration and large axons without myelin were occasionally observed. Electron microscopy observation revealed the presence of unmyelinated fibers with demyelinated axons (Figure 2).

3.5 | Genetic analysis and molecular modelling

Initial molecular analysis of known CMT-associated genes, performed with a combination of NGS panel and MLPA, was negative. Therefore, WES was performed on the proband and his parents. The analysis

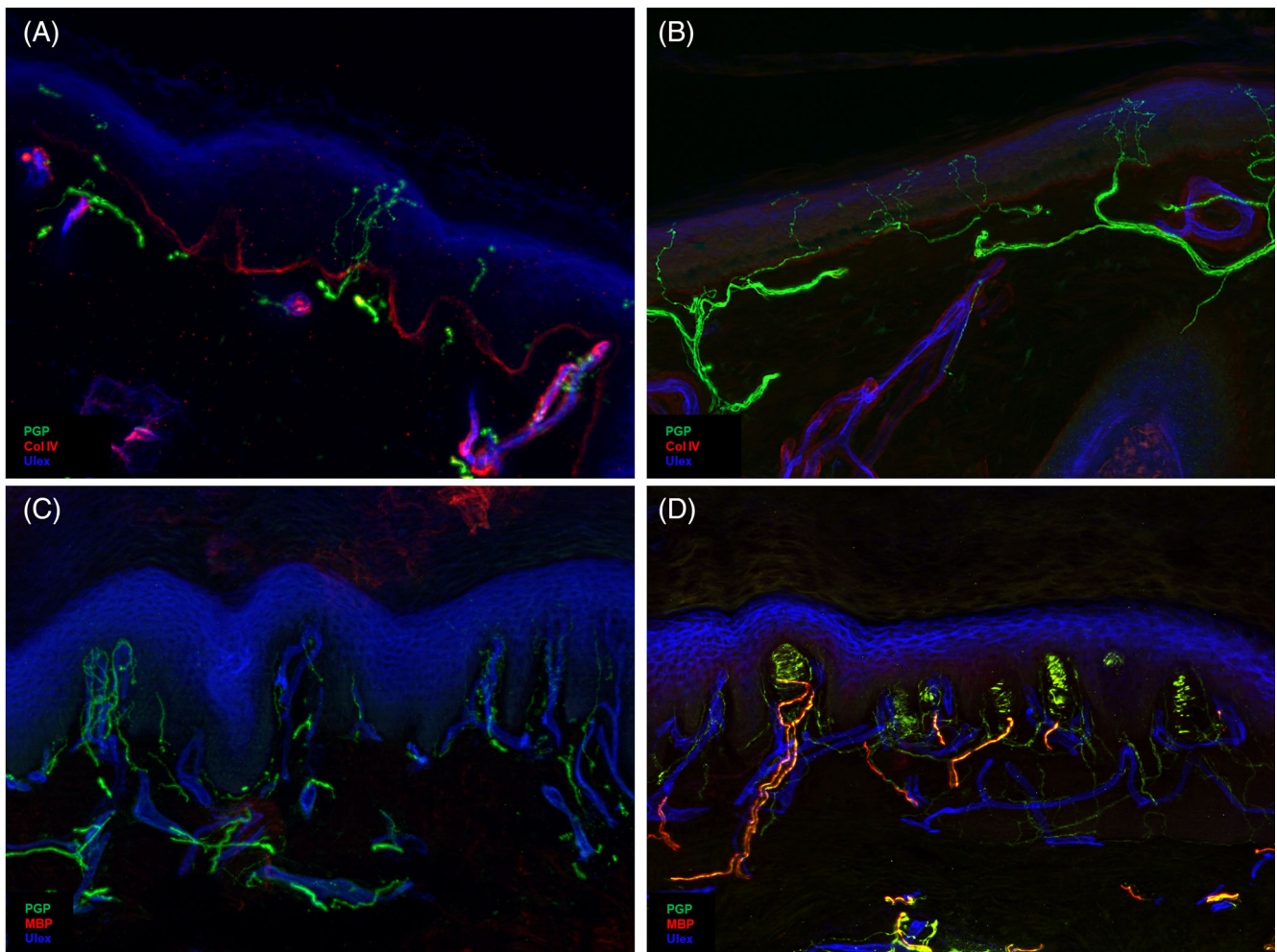


FIGURE 1 Study of skin innervation. (A and B) Digital confocal images from a distal site show a severe reduction in epidermal and dermal innervation in the patient carrying POL3RB variant (A) compared to a healthy control (B). In green: nerves marked with the pan-neuronal protein gene product 9.5 (PGP9.5) antibody; in red: basement membrane and blood vessels marked with Collagen IV (Col IV) antibody; in blue: endothelia and epidermis marked with ULEX europaeus. (C and D) Digital confocal images from fingertip of V digit show a complete absence of dermal myelinated fibres and Meissner corpuscles at the apex of dermal papillae in the patient carrying the POL3RB variant (C) respect a healthy control (D). In green: nerves marked with the pan-neuronal PGP9.5 antibody; in red: myelin sheath marked with myelin basic protein (MBP) antibody; in blue: endothelia and epidermis marked with ULEX europaeus.

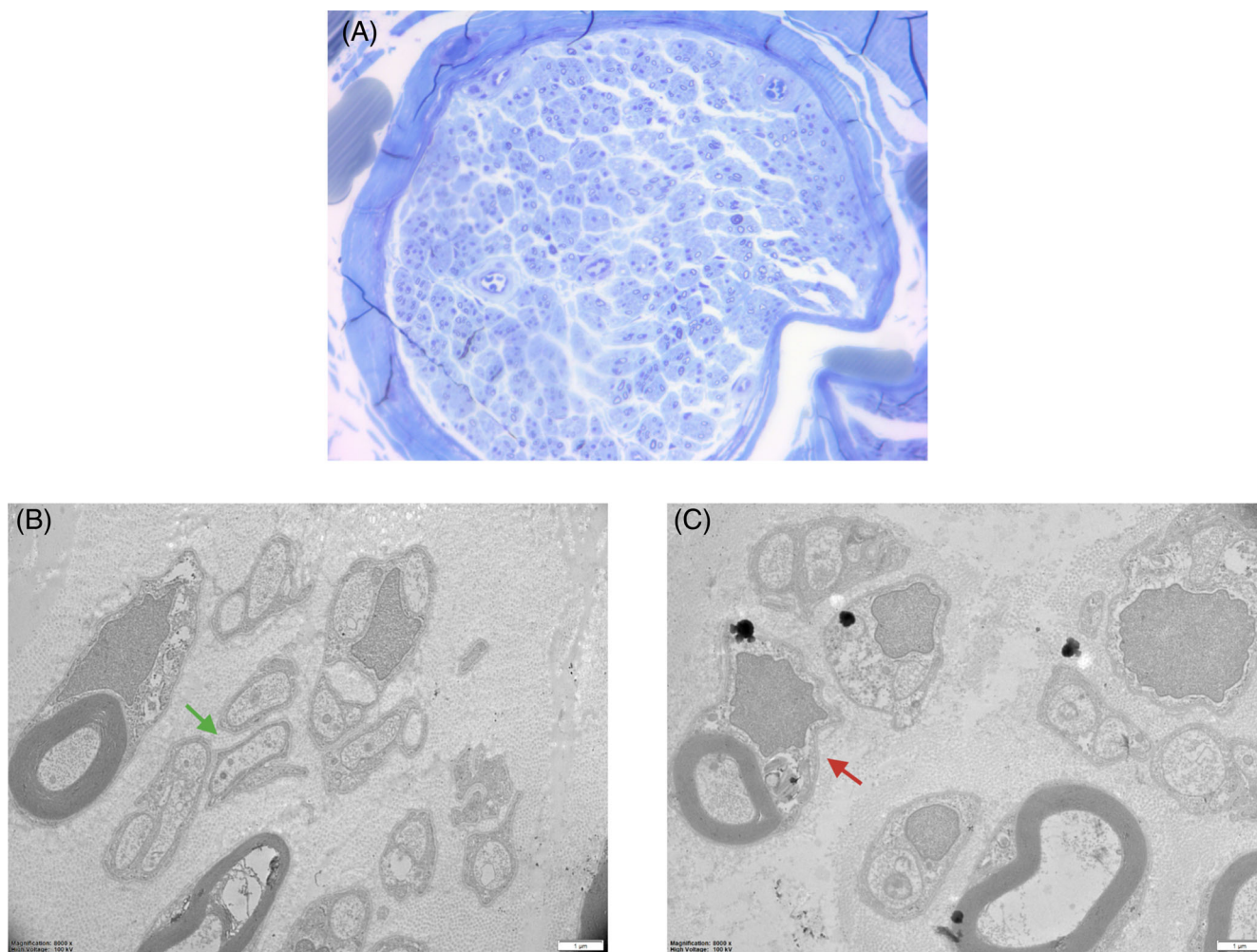


FIGURE 2 (A) Transversal section of sural nerve stained with toluidine blue at light microscope. Evident loss of large, myelinated fibers and preservation of small caliber ones. (B and C) Electron microscopy images showing amyelinated fibers with demyelinated axons (green arrow) and axonal degeneration (red arrow).

revealed a novel transition c.3136C>T (p.Arg1046Cys) in *POLR3B*. This was a de novo variant, confirmed by parental SNP analysis through analysis, never reported in the gnomAD database (Sanger validation Figure 3).

The highly conserved p.Arg1046 residue has been previously described to be involved in *POLR3B* related CMT (p.Arg1046His).^{5,6} Both changes are predicted to be deleterious by the prediction tool Revell and thus the *POLR3B* c.3136C>T variant is classified as Probably Pathogenic according to the ACMG/AMP guidelines (PS2, PM2, PM5, PP3 criteria activated).

According to cryo E.M. data, Arg1046 in *POLR3B* is involved with its side chain in two H-bonds with residues Arg353 and Gly354 backbone. In addition, its stabilizing action on the tertiary structure of the protein is enhanced by a strong salt bridge, performed by one of the side chains guanidinic nitrogens and a DNA phosphate group. The mutation suggests that this interaction is altered since a polar residue with basic features is replaced by a polar residue with slightly acid features. The Cys residue, with its most probable rotamer, can keep only one of the H-bonds formed by Arg residue, the one with the DNA phosphate group, while the salt bridge is lost. This results in a different packing in the 3D structure of the

protein, which is more prone to misfolding, is obtained (Figure 4). These computational findings are thus in agreement with the experimental data and suggest that the mutation has a deleterious effect on the protein function, accounting for the pathological condition observed in our patient.

4 | DISCUSSION

Heterozygous mutations in *POLR3B* have been described worldwide in association with peripheral neuropathies, with no apparent geographical clustering.

So far, only 10 cases have been described. The associated phenotypes described are quite heterogeneous but share the early onset phenotype and most of them showed apparently demyelinating neuropathological features.⁶

The patient described here had a pure peripheral nervous system (PNS) phenotype, as in the cases described by Djordjevic and Xue.^{6,7} Our patient showed an early onset with a peculiar concomitant weakness and atrophy of the anterior and posterior leg muscles and intrinsic hand

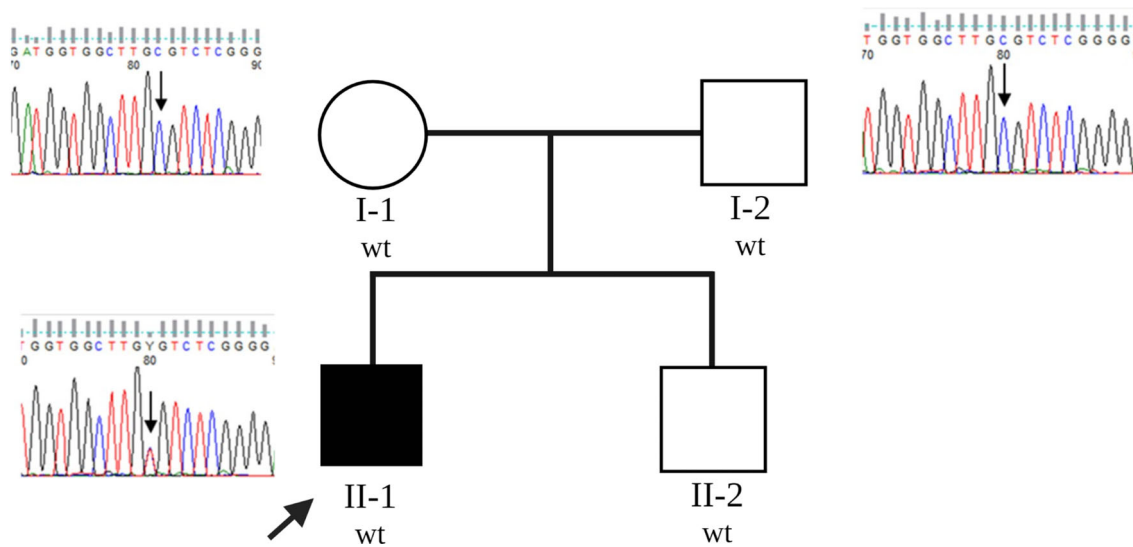


FIGURE 3 Family pedigree and Sanger validation.

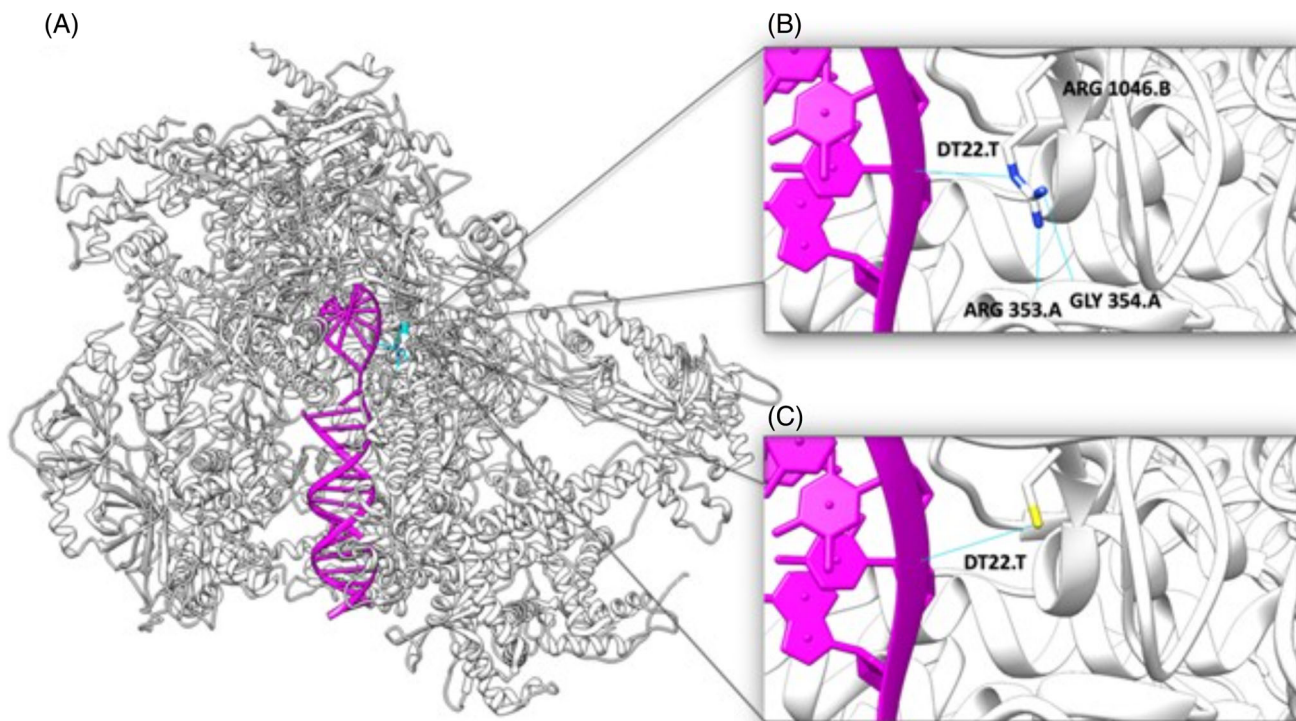


FIGURE 4 (A) Overall view of human POLR3 structure. DNA chain is depicted in magenta, while Arg1046 is colored in cyan. (B) Close up view of Arg1046 involved in the mutation. The residue is shown in stick, H-bonds are reported as cyan lines. (C) Close up view of the new variant Arg1046Cys. The residue is shown in stick, and H-bonds are reported as cyan lines.

muscles. Although the nerve conduction study in distal segments showed a severe reduction of CMAP with a MNCV slowing in demyelinating range, the study of proximal segments showed normal CMAP and MNCV, thus suggesting an axonal neuropathy. The apparent demyelinating features in the distal segment could be related to the predominance of small caliber fiber nerves. In fact, both skin and sural biopsy showed a predominant involvement of large caliber myelinated fibers in the absence of demyelination features, as previously shown by Ando et al.⁸ In conclusion,

we can hypothesize that heterozygous POLR3B-related neuropathy causes a predominant involvement of large, myelinated nerve fibers and, as occurs in other CMT types,¹⁴ the relatively small axonal caliber fibers sparing may explain the slow conduction velocities. Moreover, we cannot exclude that peripheral involvement was asymmetrical (e.g., multiplex neuropathy) as occurs in some leukodystrophies¹⁵ (Sedel), since bilateral examination was not performed. However, on neurological examination, no asymmetric involvement was evident. Finally, although the *POLR3B*

TABLE 2 Literature overview.

| Variant | Reference | Onset/age at last evaluation | Origin | Neuropathy ^a | Cerebellar signs | Intellectual disability | Brain MRI | Additional features |
|--------------------------|--------------------------------|------------------------------|------------------|-----------------------------------|------------------|-------------------------|----------------------------|---|
| c.1087G>A (p.Glu363Lys) | Djordjevic et al. ⁶ | 7/8 | Western Europe | Intermediate | Yes | Moderate | Normal | Seizures |
| c.1094C>T (p.Ala365Val) | Djordjevic et al. ⁶ | Unknown onset/22 | Irish/French | Axonal | Yes | Moderate | White matter abnormalities | Seizures, oromotor dyspraxia, progressive dysphagia |
| c.1124C>T (p.Asp375Val) | Djordjevic et al. ⁶ | 3.5/16 | East Indian | Axonal | Yes | Severe | Mild cerebellar atrophy | No |
| c.1277C>T (p.Leu426Ser) | Djordjevic et al. ⁶ | 4/4 | Turkish | Normal (only lower limb nerve) | No | Yes | Normal | Seizures |
| c.1385C>G (p.Thr462Arg) | Djordjevic et al. ⁶ | 6/14 | Scottish/English | Intermediate | Yes | Severe | Normal | No |
| c.1405C>T (p.Arg469Cys) | Ando et al. ⁸ | 10/36 | Japanese | Demyelinating | No | No | Mild cerebellar atrophy | Scoliosis |
| c.1469G>A (p.Cys490Tyr) | Ando et al. ⁸ | 2/8 | Japanese | Demyelinating | No | No | Not reported | No |
| c.3136C>T (p.Arg1046Cys) | This study | 12/19 | Italian | Axonal | No | No | Normal | No |
| c.3137C>T (p.Arg1046His) | Xue et al. ⁷ | 5/19 | Chinese | Intermediate | No | No | Normal | No |
| c.3137C>T (p.Arg1046His) | Djordjevic et al. ⁶ | 7/11 | Northern Europe | Demyelinating (no data available) | No | No | Chiari I malformation | No |

Abbreviation: MRI, magnetic resonance imaging.

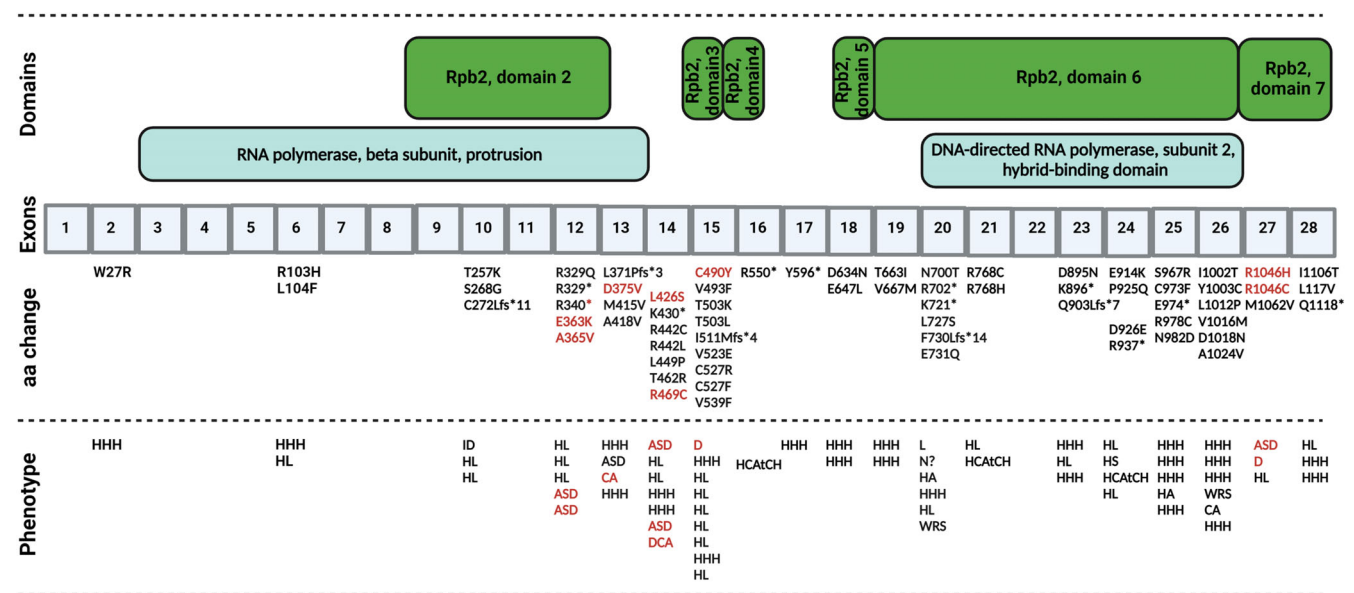
^aInterpretation of neuropathy according Berciano.

FIGURE 5 (A) POLR3B domains. (B) POLR3B variants described so far were listed and their relative phenotypes. In red heterozygous mutations associated with peripheral neuropathies. In black mutations associated with POLR3 related leukodystrophies. ASD, ataxia, spasticity, demyelinating neuropathy; CA, cerebellar ataxia; CHES, cerebellar hypoplasia with endosteal sclerosis; D, demyelinating neuropathy; DCA, demyelinating neuropathy, cerebellar atrophy; HA, hypothalamic amenorrhea; HCA1CH, hypomyelination, cerebellar atrophy, corpus callosum atrophy; HHH, hypomyelination, hypodontia, hypogonadotropic hypogonadism; HL, hypomyelinating leukodystrophy; ID, intellectual disability; L, leukodystrophy; N, neurological disease; WRS, Wiedemann Rautenstrauch Syndrome.

mutations are typically associated with a demyelinating neuropathy, the re-evaluation of the available electrophysiological data (see Table 2) according to Berciano supported that in 70% of the described cases the neuropathy was in the axonal/intermediate range rather than demyelinating. Our case reinforces that in the instance of a reduced conduction velocity in the distal nerve segment with a severe CMAP reduction, the study of a proximal segment must be performed in order to better clarify the main pathology of CMT.²

Another interesting point is the involvement of the CNS. In our case, there were no signs or symptoms of CNS involvement, and the brain MRI was normal. However, CNS Involvement could be seen as a link between POLR3B related leukodystrophies and POLR3B peripheral neuropathies. The reason why POLR3B pathogenetic variants lead to leukodystrophies or peripheral neuropathies is still unclear. To our knowledge, the variants described so far do not share between two clinical phenotypes.⁶ The position of the variants in the secondary structure of the protein or in the space, with tertiary and quaternary conformation, does not reveal any obvious cluster that could provide a domain-dependent explanation (Figure 5).

Evaluating all the variants, it seems that *POL3B-related* leukodystrophies are usually caused by the association of a nonsense and a missense mutation, less frequently by two missense mutations, while the association of two nonsense mutations has never been described.⁵ These data may suggest a partial loss of function (LOF) mechanism, whereas complete loss of the protein is unlikely to be viable. In contrast, the CMT phenotype is always associated with de novo missense mutations. Djordjevic et al. showed that leukodystrophy-associated mutations cause a complete disassembly of the polymerase, whereas CMT-associated variants seem to affect only the binding to single RNAPol3 subunits. A dominant-negative effect has been suggested and so we can postulate a broader LOF mechanism, where polymerase functionality is progressively lost. Heterozygous missense mutations are likely to cause an impaired function with a dominant-negative effect, while the compound heterozygous ones lead to a severe LOF.

Until today, variants involving the Arg1046 residue are the only ones that interact directly with DNA through H-bonds. The aminoacidic change p.Arg1046Cys, reported here, may cause the loss of two H-bonds with the POLR3A subunit. The binding to DNA remains, but changes from NH to SH binding. On the contrary, the already described p.Arg1046His leads to the loss of all the H-bonds. Interestingly, these two aminoacidic changes are the only ones associated with a pure neuropathy. Also, a patient with the p.Cys490Tyr variant described by Ando et al. has a neuropathy, but without a brain MRI to exclude any CNS involvement.

The reasons why recessive mutations have an exclusive CNS involvement whereas heterozygous de novo mutations have a predominant PNS involvement is still unclear. The absence of any peripheral involvement in patients with POLR3B-related leukodystrophy, but also in their healthy reported parents, adds to the confusion.

Could the perhaps mild neuropathy, be overshadowed by the more severe clinical phenotype of leukodystrophy? Or is one variant in the *POLR3B* gene not enough and a hidden second event is needed

to make the pathogenicity of a single *POLR3B* mutation effective? All these questions need to be answered in the future.

The allelic heterogeneity of *POLR3B* is also critical in genetic counseling. Is the heterozygous *POLR3B* neuropathic patient also a carrier of leukodystrophy? The classification of the variants into two subgroups seems to give us a negative answer, but the number of the described variants is still too small to answer this question definitely. If in the future, a positive answer can be demonstrated, the question of offering a *POLR3B* carrier test in a couple, will arise despite the very low frequency of mutation.⁸

5 | CONCLUSION

We report a patient with a de novo heterozygous mutation in the *POLR3B* gene. Electrophysiological and morphological features suggest that the *POLR3B*-related neuropathy is due to a predominant involvement of large, myelinated nerve fibers and the least involvement of small caliber fibers may explain the slow conduction velocities previously misinterpreted as demyelinating neuropathy.

ACKNOWLEDGEMENTS

Thanks to the patient and his family and to ACMT-Rete and Gruppo CMT per AIGEM Onlus for all the support.

CONFLICT OF INTEREST STATEMENT

The authors declare no conflict of interest.

DATA AVAILABILITY STATEMENT

The data that support the findings of this study are available from the corresponding author upon reasonable request.

ORCID

Alessandro Geroldi  <https://orcid.org/0000-0002-2208-9195>

Stefano Tozza  <https://orcid.org/0000-0002-9672-4577>

REFERENCES

1. Braathen GJ, Sand JC, Lobato A, Høyer H, Russell MB. Genetic epidemiology of Charcot-Marie-Tooth in the general population. *Eur J Neurol.* 2011;18:39-48.
2. Berciano J, García A, Gallardo E, et al. Intermediate Charcot-Marie-Tooth disease: an electrophysiological reappraisal and systematic review. *J Neurol.* 2017;264(8):1655-1677.
3. Saitsu H, Osaka H, Sasaki M, et al. Mutations in POLR3A and POLR3B encoding RNA polymerase III subunits cause an autosomal-recessive hypomyelinating leukoencephalopathy. *Am J Hum Genet.* 2011;89(5):644-651.
4. Lata E, Choquet K, Saggiocco F, Brais B, Bernard G, Teichmann M. RNA polymerase III subunit mutations in genetic diseases. *Front Mol Biosci.* 2021;8:696438.
5. Tetreault M, Choquet K, Orcesi S, et al. Recessive mutations in POLR3B, encoding the second largest subunit of pol III, cause a rare hypomyelinating leukodystrophy. *Am J Hum Genet.* 2011;89(5):652-655.
6. Djordjevic D, Pinar M, Gauthier MS, et al. De novo variants in POLR3B cause ataxia, spasticity, and demyelinating neuropathy. *Am J Hum Genet.* 2021;108(1):186-193.

7. Xue YY, Cheng HL, Dong HL, et al. A de novo variant of POLR3B causes demyelinating Charcot-Marie-Tooth disease in a Chinese patient: a case report. *BMC Neurol*. 2021;21(1):402.
8. Ando M, Higuchi Y, Yuan JH, et al. Novel de novo POLR3B mutations responsible for demyelinating Charcot-Marie-Tooth disease in Japan. *Ann Clin Transl Neurol*. 2022;9(5):747-755.
9. Provitera V, Nolano M, Caporaso G, Stancanelli A, Santoro L, Kennedy WR. Evaluation of sudomotor function in diabetes using the dynamic sweat test. *Neurology*. 2010;74(1):50-56.
10. Tozza S, Severi D, Palumbo G, et al. Quantitative sensory testing in late-onset ATTRv presymptomatic subjects: a single center experience. *Biomedicine*. 2022;10(11):2877.
11. Manganelli F, Parisi S, Nolano M, et al. Novel mutations in dystonin provide clues to the pathomechanisms of HSAN-VI. *Neurology*. 2017;88(22):2132-2140. doi:10.1212/WNL.0000000000003992
12. Girbig M, Misiaszek AD, Vorländer MK, et al. Cryo-EM structures of human RNA polymerase III in its unbound and transcribing states. *Nat Struct Mol Biol*. 2021;28(2):210-219.
13. Pettersen EF, Goddard TD, Huang CC, et al. UCSF Chimera—a visualization system for exploratory research and analysis. *J Comput Chem*. 2004;25(13):1605-1612.
14. Pisciotta C, Bai Y, Brennan KM, et al. Reduced neurofilament expression in cutaneous nerve fibers of patients with CMT2E. *Neurology*. 2015;85(3):228-234.
15. Sedel F, Barnerias C, Dubourg O, Desguerres I, Lyon-Caen O, Saudubray JM. Peripheral neuropathy and inborn errors of metabolism in adults. *J Inherit Metab Dis*. 2007;30(5):642-653.

How to cite this article: Geroldi A, Tozza S, Fiorillo C, et al. A novel de novo variant in *POLR3B* gene associated with a primary axonal involvement of the largest nerve fibers. *J Peripher Nerv Syst*. 2023;28(4):620-628. doi:10.1111/jns.12602